Cell Research (2011) 21:1711-1722.

www.nature.com/cr

ORIGINAL ARTICLE

The AP-3 adaptor complex is required for vacuolar function in *Arabidopsis*

Marta Zwiewka[1, 2], Elena Feraru[1, 2], Barbara Möller[3], Inhwan Hwang[4], Mugurel I Feraru[1, 2], Jürgen Kleine-Vehn[1, 2], Dolf Weijers[3], Jiří Friml[1, 2]

[1]Department of Plant Systems Biology, VIB, Technologiepark 927, 9052 Gent, Belgium; [2]Department of Plant Biotechnology and Genetics, Ghent University, Gent, Belgium; [3]Laboratory of Biochemistry, Wageningen University, Wageningen, The Netherlands; [4]Division of Integrative Biosciences and Biotechnology, Pohang University of Science and Technology, Pohang, Korea

Subcellular trafficking is required for a multitude of functions in eukaryotic cells. It involves regulation of cargo sorting, vesicle formation, trafficking and fusion processes at multiple levels. Adaptor protein (AP) complexes are key regulators of cargo sorting into vesicles in yeast and mammals but their existence and function in plants have not been demonstrated. Here we report the identification of the *protein-affected trafficking 4* (*pat4*) mutant defective in the putative δ subunit of the AP-3 complex. *pat4* and *pat2*, a mutant isolated from the same GFP imaging-based forward genetic screen that lacks a functional putative AP-3 β, as well as dominant negative AP-3 μ transgenic lines display undistinguishable phenotypes characterized by largely normal morphology and development, but strong intracellular accumulation of membrane proteins in aberrant vacuolar structures. All mutants are defective in morphology and function of lytic and protein storage vacuoles (PSVs) but show normal sorting of reserve proteins to PSVs. Immunoprecipitation experiments and genetic studies revealed tight functional and physical associations of putative AP-3 β and AP-3 δ subunits. Furthermore, both proteins are closely linked with putative AP-3 μ and σ subunits and several components of the clathrin and dynamin machineries. Taken together, these results demonstrate that AP complexes, similar to those in other eukaryotes, exist in plants, and that AP-3 plays a specific role in the regulation of biogenesis and function of vacuoles in plant cells.

***Keywords*:** AP-3 complex; PSVs; protein trafficking; vacuole biogenesis and function

Cell Research (2011) **21**:1711-1722. doi:10.1038/cr.2011.99; published online 14 June 2011

Introduction

Diverse types of cargos are sorted and transported by coated vesicles to multiple destinations in eukaryotic cells. Vesicles that bud from a donor membrane are subsequently fused with a target membrane. The process of vesicle budding is initiated by the recruitment of specific regulators from the cytosol onto the donor membrane. One set of proteins form a coat that can function as a scaffold enabling physical membrane deformation, and another can determine vesicle composition by interacting with cytosolic domains of transmembrane proteins. Proteins linking cargos with the coat proteins form complexes known as adaptor protein (AP) complexes [1-3].

APs are key regulators of protein sorting into vesicles. Four different heterotetrameric AP complexes (AP-1 to AP-4) have been characterized so far in eukaryotes including yeast, *Drosophila* and mammals. Each AP is composed of four subunits, also called adaptins: two large subunits (γ/α/δ/ε and β1-β4), a medium subunit (μ1-μ4) and a small subunit (σ1-σ4). The best-known complexes in vesicle formation and budding are the complexes made of clathrin and APs, such as AP-1 and AP-2. AP complexes are recruited from the cytosol and required for sorting and concentration of cargos into the coated pits, as well as for the recruitment of clathrin to the membranes. The AP-2 complex mediates the formation of clathrin-coated vesicles for endocytosis from the plasma membrane (PM) to trans-Golgi network/early endosomes (TGN/EEs), while AP-1 functions in clathrin-

Correspondence: Jiří Friml
Tel: +32 (0) 9-33-13-800; Fax: +32 (0) 9-33-13-809
E-mail: jiri.friml@psb.vib-ugent.be
Received 21 December 2010; revised 11 February 2011; accepted 17 March 2011; published online 14 June 2011

dependent sorting at the TGN/EEs. In contrast, it appears that AP-3 and AP-4 might at least partially function independently of clathrin [3, 4].

The AP-3 complex is one of the most recently identified complexes in organisms such as yeast, flies and mammals and it has been found to play a role in protein sorting at the TGN and/or endosomes [5-8]. The AP-3-mediated trafficking to the vacuole (in yeast) or lysosomes and lysososome-related organelles (flies and mammals) is supposed to bypass the classical vacuolar trafficking route, which most vacuolar cargos use and that involves late endosomes/prevacuolar compartments multivesicular bodies/(LE/PVC/MVB'S) [5, 6, 8, 9]. Recently, we have shown that the putative AP-3 β protein plays a role in vacuolar function in *Arabidopsis,* including mediation of the transition between storage and lytic vacuolar identity [10]. In addition, several putative AP-3 adaptins have been identified as suppressors of *zigzag 1* (*zig1*) [11], a mutant affecting a vesicle trafficking regulator, the SNARE VTI11 [12, 13]. Nonetheless, the existence and function of AP complexes, including AP-3, has not been demonstrated in plants.

In the present study, we present the identification and characterization of *pat4*, a mutant defective in the AP-3 δ adaptin, as well as the identification and genetic and biochemical characterization of the AP-3 complex in *Arabidopsis*. Our observations strongly suggest that an AP-3 complex exists in plants and together with clathrin and dynamin-like proteins is required for function of lytic and protein storage vacuoles (PSVs) in *Arabidopsis*.

Results

Identification of the protein-affected trafficking4 (pat4) mutant

As an approach to identify new regulators of protein trafficking pathways we carried out a fluorescence imaging-based forward genetic screen for mutants affecting the subcellular trafficking of the PIN1 auxin efflux carrier [14], which undergoes elaborate subcellular dynamics including secretion [15], clathrin-mediated endocytosis [16], polar recycling [17, 18] and trafficking to the vacuole [19, 20]. By using an ethyl methanesulfonate (EMS)-mutagenized $PIN1_{pro}$*:PIN1-GFP* population we originally identified three independent *pat* mutant loci from about 1 500 M1 families; among them *pat2-1* is defective in the putative β adaptin of the AP-3 complex [10]. In a further genetic screen using the progeny of other 1 920 M1 families we identified two additional non-allelic mutants *pat4* and *pat5*. *pat4-1* is a recessive mutant showing strong defects in subcellular trafficking of PIN1-GFP (Figure 1A and 1B). In addition to its normal basal localization in root stele cells, we observed strong intracellular accumulations (Figure 1A and 1B). Similarly, other polar (PIN2 [21]), apolar (PIP2 aquaporin [22] and BRI1 brassinosteroid receptor [23]) PM proteins showed aggregation in intracellular compartments (Figure 1C-1H).

The pronounced intracellular accumulation of diverse proteins had surprisingly little impact on the plant morphology because *pat4-1* did not show any abnormal phenotypes under standard growth conditions (Supplementary information, Figure S1A and S1B). However, about 40% of *pat4-1* seedlings, when grown on medium lacking sucrose, showed arrested growth at the seedling stage (Figure 1I and 1J). In addition, the germination capacity of *pat4* mutant seeds decreased strongly with time of storage as compared to control (not shown).

Thus, a PIN1-GFP-based forward genetic screen identified the *pat4* mutant showing almost normal growth and morphology but pronounced changes in subcellular

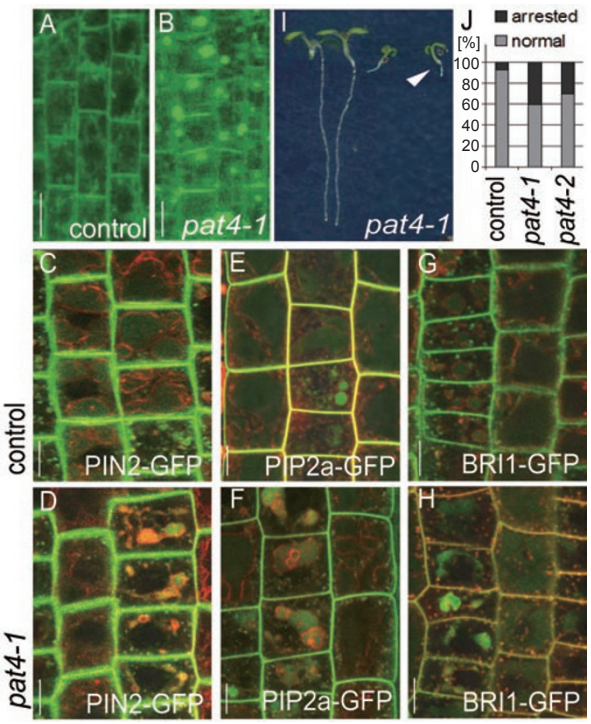

Figure 1 Ectopic, intracellular accumulation of plasma membrane proteins in *pat4-1* mutant. **(A-H)** Polar plasma membrane proteins PIN1-GFP **(A**, **B)** and PIN2-GFP **(C**, **D)** as well as apolar proteins PIP2a-GFP **(E**, **F)** and BRI1-GFP **(G**, **H)** showed strong intracellular accumulations in *pat4-1* mutant seedlings **(B**, **D**, **F**, **H)** compared to control seedlings in wild-type background **(A**, **C**, **E**, **G)**. **(I**, **J)**. *pat4-1* seedlings showing growth arrest **(I**, arrowhead**)** on medium without sucrose. The chart **(J)** depicts percentage of arrested seedlings in *pat4-1* and *pat4-2* mutant lines. Scale bar = 10 μm.

distribution of different PM proteins.

pat4 mutants show normal endocytosis and recycling

Next, we investigated which trafficking pathway might be affected by the *pat4* mutation, and in which subcellular compartment(s) the ectopic accumulation of proteins in *pat4* mutants occurs. In *Arabidopsis* roots, treatment with Brefeldin A (BFA) leads to internalization of PM proteins including PIN1-GFP into so-called BFA compartments that consist of aggregated TGN/EEs and recycling endosomes with Golgi apparatus (GA) at their periphery [17, 24-26]. A 1 h treatment with 50 μM BFA, combined with PM labeling by 4 μM endocytic tracer FM4-64 [27] led to a rapid internalization of PM-localized PIN1-GFP and its colocalization with FM4-64-stained BFA compartments (Figure 2A) indicating that constitutively cycling PIN1-GFP accumulates in endosomal aggregations. In *pat4-1* roots, the early stages of FM4-64 uptake, as well as the effect of BFA, were comparable to the control. Besides the BFA compartments defined as a colocalization of PIN1-GFP signal with FM4-64 (Figure 2A and 2B), we also observed additional PIN1-GFP aggregations that were not stained with FM4-64 (Figure 2B) and corresponded to ectopic PIN1-GFP aggregations in the untreated *pat4-1* roots (Figure 1A and 1B). Furthermore, the abundance of PIN1-GFP at the basal PM in the *pat4-1* mutant was comparable to the control PIN1-GFP line (Figure 4G). This result is also consistent with a notion that secretion, endocytosis and recycling were not affected in *pat4-1* mutant root cells.

From this observation we concluded that endocytosis and recycling were not significantly affected in the *pat4-1* mutant and that the ectopic PIN1-GFP accumulation does not occur in the early compartments of the endocytic pathway since all these are associated with BFA compartments.

pat4 mutants accumulate proteins in aberrant lytic vacuoles

During internalization, the endocytic tracer FM4-64 labels the EEs, subsequently it marks intracellular compartments and finally it reaches the vacuole and labels the vacuolar membrane, the tonoplast [28]. In the *pat4-1* mutant after long treatment (3 h) with 4 μM FM4-64, the dye stained the ectopic intracellular accumulations of PIN1-GFP (Figure 2C and 2D). This result suggests a late endosomal/vacuolar identity of PIN1-GFP aggregations in the *pat4-1* mutant.

Staining of the tonoplast with FM4-64 also revealed an aberrant morphology of vacuoles in the *pat4* mutant (Figure 2G-2L). To confirm this observation, we performed a 1 h treatment with the fluorescent acidotro-

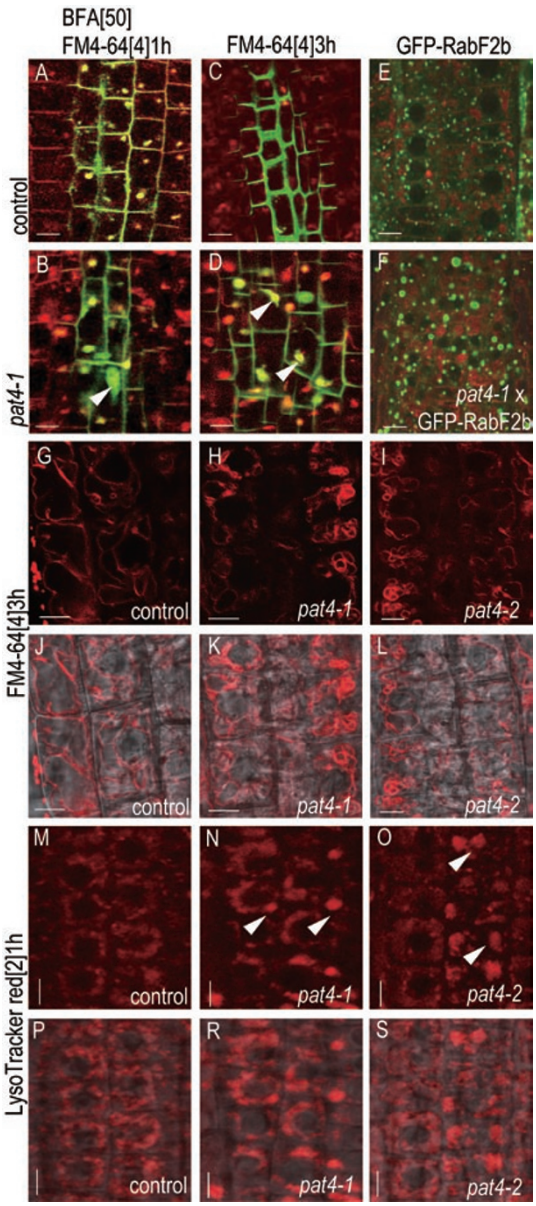

Figure 2 Impaired morphology and biogenesis of lytic vacuole in *pat4* mutants. **(A-D)** PIN1-GFP-expressing seedlings in wild type **(A**, **C)** and *pat4-1* mutant background **(B**, **D)** stained with FM4-64 and co-treated with 50 μM BFA for 1 h **(A**, **B)**. Untreated seedlings were stained with FM4-64 for 3 h **(C**, **D)**. Note the PIN1-GFP aggregations in *pat4-1* **(B**, arrowheads**)** were distinct from BFA compartments **(B**, yellow compartments**)**. Only after long incubation (3 h), FM4-64 stained PIN1-GFP-containing compartments in the stele cells of *pat4-1* **(D**, arrowheads**)**. The localization of GFP-RABF2b **(E**, **F)** revealed strong enlargement of the late endosomes/PVCs in *pat4-1* **(F)** as compared to the control **(E)**. After 3 h, FM4-64 stained the tonoplast of root epidermal cells in control **(G**, **J)** and revealed misshaped vacuoles in *pat4-1* **(H**, **K)** and *pat4-2* **(I**, **L)** mutants. **(M-S)** LysoTracker red accumulation in the vacuoles of root epidermal cells. Stronger dye accumulation in *pat4-1* **(N**, arrowheads**)** and *pat4-2* **(O**, arrowheads**)** indicate changed vacuolar identity. Scale bar = 5 μm **(A)** to **(F)** and 10 μm **(G)** to **(S)**.

pic probe Lysotracker red (2 μM), which labels acidic compartments including PVC and vacuole [29]. The staining pattern of this probe in the root cells of *pat4* mutants showed pronounced differences as compared to the control (Figure 2M-2S). The provacuole-like tubular extensions typically visible in the control [30], were largely absent in the *pat4* mutant, and the labeling with the probe was generally visibly stronger (Figure 2N, 2O, 2R and 2S). These findings suggest that lytic vacuoles in *pat4* mutant cells have the aberrant morphology and ectopically accumulate proteins, which normally undergo vacuole-mediated degradation.

Next, we analyzed whether the *pat4* mutation has an effect on the morphology of PVCs, which are known to function upstream of lytic vacuoles [31-33]. In the *pat4* mutant background, we observed swelling and vacuolization of PVC compartments visualized by PVC markers, such as GFP-RABF2b [34] (Figure 2E and 2F). Moreover, the swollen PVC phenotype in the *pat4* mutant resembled the effect of wortmannin on the PVC morphology [10]. Taken together, these results indicate that aberrant vacuole-like compartments in *pat4* mutants can share features of both PVCs and vacuoles. This mixed identity is presumably linked to defects in function of lytic vacuoles, which cause the ectopic accumulation of cargos in aberrant vacuoles.

pat4 mutants show defects in seed PSVs

The *pat4* mutant does not show any striking morphological phenotype. However, seedlings germinated on medium lacking sucrose regularly showed developmental arrest (Figure 1I and 1J). This is typical for mutants with defects in PSVs [10, 20, 35-37]. In seeds, PSVs accumulate high amounts of reserve proteins such as albumins and globulins that serve as a source of energy during germination. The majority of mutants defective in PSVs function display ectopic sorting of these proteins to the extracellular space, which is reflected by defective maturation of these proteins and accumulation of unprocessed precursors [13, 35, 38]. PSVs in seeds of the *pat4* mutant were smaller, more fragmented and very often spherically shaped in comparison with the control (Figure 3A, 3B 3G and Supplementary information, Figure S4A-S4C). Therefore, we investigated whether the observed defects in PSVs morphology are associated with defects in sorting of storage proteins. However, we could not detect any defect in the processing of 2S albumin and 12S globulin storage proteins since the precursors of these proteins did not accumulate in the dry seeds of *pat4* as revealed by western blot analysis of these proteins. This is in contrast to known mutants defective in PSVs such as *vps29* [35] that accumulate precursors of storage proteins (Figure 3H and 3I). This result shows that, despite morphological defects of PSVs in the *pat4* mutant, the sorting and delivery of storage proteins to PSVs is unaffected.

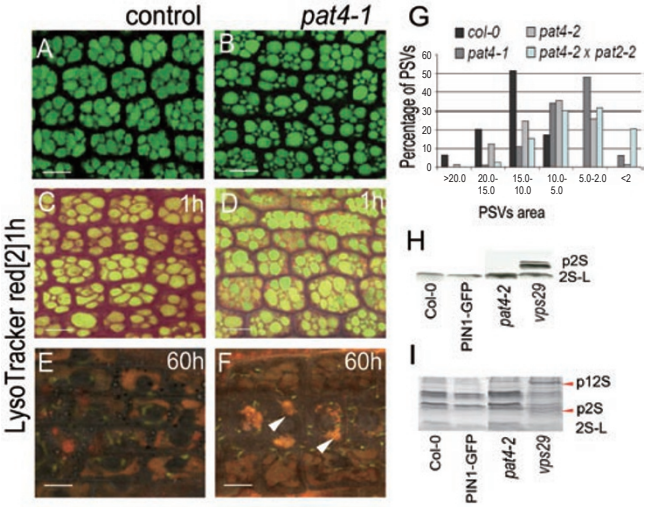

Figure 3 Defects in the transition between PSVs and lytic vacuoles, but not in trafficking to the PSVs in *pat4* mutants. **(A-B)** PSVs in embryo root cells of control **(A)** and *pat4-1* **(B)**. **(C-F)** Accumulation of LysoTracker red following 1 h **(C, D)** and 60 h **(E, F)** of imbibition in wild-type **(C, E)** and *pat4-1* **(D, F)** seeds, indicating defects in the acidification of mutant PSVs. **(G)** Quantification of the PSVs morphology. *pat4-1* mutant (gray bar), *pat4-2* mutant (light gray bar) and double mutant *pat4* × *pat2* (light blue bar) show smaller PSVs compared to wild-type seeds (black bar). Western blot **(H)** and SDS-PAGE **(I)** revealed no missecretion of 2S albumin and 12S globulin precursors in *pat4-2* mutant but accumulation in the *vps29*, a mutant known to missort reserve proteins. Scale bar = 10 μm.

A time-course visualization of PSVs revealed that *pat4* mutants are defective in the morphology of storage vacuoles (Supplementary information, Figure S2A-S2F). In control seeds, 60 h following germination, almost all storage proteins were degraded and PSVs showed only weak remaining autofluorescence (Supplementary information, Figure S2B). In contrast, in *pat4* seeds, regions of strong autofluorescence were still observed after the same time post-germination demonstrating persisting accumulation of storage proteins, which could be the result of the flawed structure of PSVs (Supplementary information, Figure S2D and S2F). Accordingly, the time-course of LysoTracker red staining in germinating seeds showed abnormal acidification in *pat4-1* confirming delayed transition of *pat4-1* PSVs into lytic vacuoles following germination (Figure 3C-3F). Overall, these results show the aberrant morphology and the defective transition of PSVs into lytic vacuoles in the *pat4* mutants.

PAT4 encodes the δ subunit of the AP-3 complex

The *pat4* mutant is defective in the vacuolar function and displays a number of unique features that are shared by only one other characterized mutant – *pat2* – that is defective in the function of the putative β subunit of the AP-3 complex [10]. All developmental, as well as cellular phenotypes of the *pat4* mutant including normal trafficking of reserve proteins to PSVs are strongly reminiscent of the *pat2* mutant. This suggests that *pat4* and *pat2* are defective in the same process. To test whether these mutants represent alleles of the same mutation, we performed allelism test and analyzed F1 seedlings of the cross between *pat4-1* and *pat2-2*. The F1 seedlings showed a complete rescue of the cellular phenotype present in both parental lines (Figure 4C, 4D and 4F) confirming the recessive character and different identity of both mutations.

To gain insight into the molecular nature behind the vacuolar defect of *pat4-1* we mapped the mutation by positional cloning using 300 chromosomes from the F2 progeny derived from crosses of *pat4-1* with the Landsberg *erecta* ecotype. Sequencing the candidate genes within the interval, we found a point mutation 223 nucleotides after the ATG resulting in a premature stop codon in the gene coding for a putative δ subunit of the AP complex AP-3 (Figure 4A and 4B). The stop codon at the beginning of the coding sequence leads to the truncation of more than 90% of the predicted full-length protein strongly suggesting that *pat4-1* is a loss-of-function mutation.

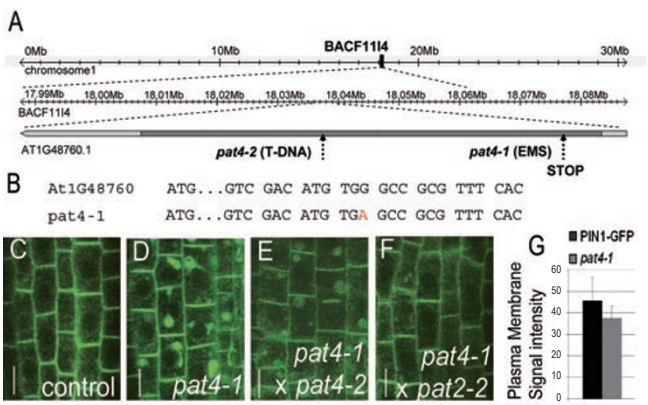

Figure 4 PAT4 encodes AP-3 δ adaptin. **(A)** Scheme of AP-3 δ locus on chromosome 1. **(B)** The positions of the *pat4* allele and the point mutation (red letter) are depicted. **(C-F)** PIN1-GFP intracellular distribution in *PIN1::PIN1-GFP* **(C)**, *pat4-1* **(D)** and F1 crosses between *pat4-1* and the SALK line *pat4-2* **(E)** or *pat4-1* and *pat2-2* **(F)**. **(G)** The chart depicts intensity of PIN1-GFP signal at the PM of root stele cells in *pat4-1* compared to the PIN1-GFP line. Error bars represent SD. Scale bar = 10 μm.

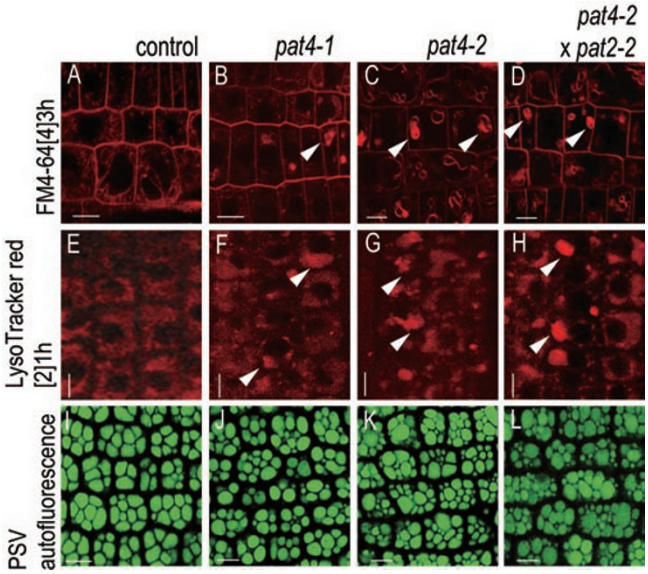

Figure 5 Vacuole morphology in *pat4-2* × *pat2-2* double mutants. **(A-D)** FM4-64 uptake (3 h) in control **(A)**, *pat4-1* **(B)**, *pat4-2* **(C)** and *pat4-2* × *pat2-2* double mutant **(D)**. Similarly to the single *pat4* mutants, the vacuole morphology in the double mutant was impaired (arrowheads). **(E-H)** LysoTracker red accumulation in control **(E)**, *pat4-1* **(F)**, *pat4-2* **(G)** and *pat4-2* × *pat2-2* double mutant **(H)** showed abnormal acidification and lytic vacuole morphology in the single and double mutants (arrowheads). **(I-L)** PSVs autofluorescence imaging revealing defective PSVs morphology in single *pat4-1* **(J)**, *pat4-2* **(K)** and *pat4-2* × *pat2-2* double mutants **(L)** as compared to wildtype embryos **(I)**. Scale bar = 10 μm.

To confirm this, we analyzed an additional T-DNA insertion allele (*pat4-2*) in the AP-3 δ locus that had been previously described as a full knock-out mutant based on the lack of AP-3 δ mRNA [11]. The *pat4-2* mutant showed comparable cellular and morphological phenotypes as the original *pat4-1* allele (Figures 1J, 2I, 2L, 2O, 2S, 3G, 5C, 5G, 5K and 6C, 6H). Furthermore, all F1 seedlings from the cross between the original *pat4-1* allele and the *pat4-2* T-DNA insertion line showed the same intracellular PIN1-GFP aggregation as the parental homozygous lines (Figure 4D and 4E). These findings demonstrate that the *pat4-1* and *pat4-2* are both recessive, loss-of-function alleles of the gene coding for the putative δ subunit of the presumptive AP-3 complex. The positive result of the allelic test between *pat4-1* and *pat4-2* confirmed that trafficking defect reflecting intracellular accumulation of proteins in *pat4-1*, is caused by mutation in the gene coding for the putative δ subunit of the presumptive AP-3 complex. Thus, the similar morphological and cellular defects observed in *pat2-2* and *pat4-1* mutants are caused by mutations in the putative β and δ

subunits of the same AP-3 complex.

pat2 and pat4 are defective in the same process related to vacuolar function

The identification of PAT4 coding for the putative AP-3 δ subunit reveals that the similar morphological and cellular defects observed in *pat2-2* and *pat4-1* mutants are caused by mutations in the putative β and δ subunits of the same AP-3 complex. To address the common action of the corresponding gene products, we analyzed the phenotype of the *pat4* × *pat2* double mutant. The double mutant showed the same, albeit somewhat stronger, aberrations in vacuole morphology than the *pat4* single mutant as visualized by tonoplast staining with FM4-64 (Figure 5A-5D). Similarly, staining with LysoTracker red revealed aberrations in acidification of vacuolar compartments in the double mutant (Figure 5E-5H). The PSVs of the double mutant seeds were affected in a similar way as those in each single mutant, but showed stronger fragmentation than in the single mutant seeds (Figures 3G, 5I-5L, Supplementary information, Figure S3A-S3C). The maturation of lytic vacuoles was strongly abnormal in the double mutant seeds as revealed by persisting autofluorescence of storage proteins in double mutant PSVs contrasting to wild-type germinating seeds (Supplementary information, Figure S2B and S2F). Accordingly, the transition of PSVs to lytic vacuoles was also affected as shown by LysoTracker red staining (Supplementary information, Figure S3D-S3G). These defects in PSVs maturation of the double mutants were similar, albeit slightly stronger, than in single mutants [10].

The similar phenotypes of the single mutants and lack of strong additive or synergistic interaction in the double mutant combination suggest that *pat2* and *pat4* are defective in the same process related to the biogenesis and function of lytic and storage vacuoles.

AP-3 μ subunit is required for vacuolar morphology

The similar phenotypes of mutants defective in the putative β and δ subunits of the AP-3 complex, *pat2* and *pat4*, respectively, suggest that the AP-3 complex, previously characterized in yeast and animals [1, 4-6], exists also in plants and plays a role in regulating vacuolar function.

To further test this hypothesis, we generated a dominant negative version of the putative AP-3 μ subunit by truncating 18 amino acids from its C-terminal domain that is required for cargo recruitment into the forming vesicle [39]. This strategy had been successfully used previously in animal cells to inhibit the function of the whole corresponding AP complex [40]. Vacuole staining by FM4-64 (Figure 6A-6E) or LysoTracker red (Figure 6F-6J) revealed aberrant vacuolar morphology in seedlings overexpressing the dominant negative (DN) version of the AP-3 μ subunit (35S::*AP3μ*^{DN}), similar to those observed in *pat2* and *pat4* mutants. Our findings that interference with the function of either putative AP-3 β, AP-3 δ or AP-3 μ has similar effects on morphology and function of vacuoles in plant cells suggest that these proteins act together in the same AP-3 complex. Thus AP

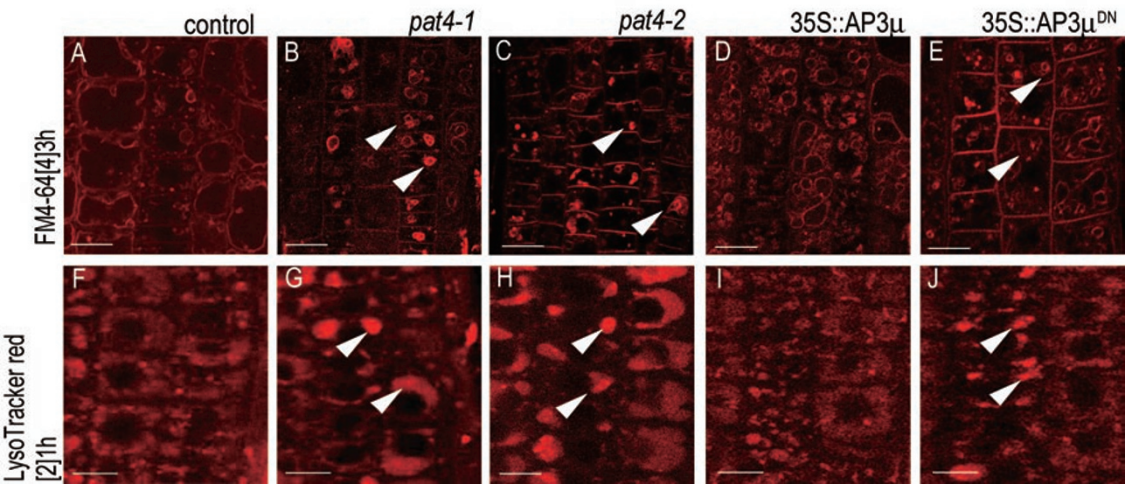

Figure 6 Defects in lytic vacuole morphology and function in *AP-3* μ dominant negative mutant. **(A-J)** FM4-64 uptake for 3 h **(A-E)** and LysoTracker staining for 1 h **(F-J)** in wild type **(A**, **F)**, *pat4-1* **(B**, **G)**, *pat4-2* **(C**, **H)**, *35S:AP3μ* **(D**, **I)** and the dominant negative (*35S:AP3μ*^{DN}) expressing root cells **(E**, **J)**. Note the similar mislabeling of FM4-64 and LysoTracker red in *pat4* mutants alleles and *AP3μ*^{DN} (arrowheads). Scale bar =10 μm.

Table 1 Identification of AP-3 β and AP- 3 δ interacting proteins from immunopreciptations of 5-day-old seedlings

AGI	Protein name	AP-3 β-GFP						AP-3 δ-GFP					
		Exp. 1			Exp. 2			Exp. 1			Exp. 2		
		N	**%**	**Sf**	***N***	**%**	**Sf**	***N***	**%**	**Sf**	***N***	**%**	**Sf**
At3g55480	AP-3 β	73	62	63	75	62	65	36	39	31	14	17	11
At1g48760	AP-3 δ	37	51	31	38	55	34	45	53	40	41	44	31
At1g56590	AP-3 μ	14	41	11	13	45	10	4	12	2.6			
At3g50860	AP-3 σ	5	39	4.4	5	39	4.1						
At5g42080	ADL1A	10	20	8.4				16	32	11			
At1g14830	ADL1C	6 (3)	12	4.9				4 (3)	7.2	3.1			
At3g60190	ADL1E	4 (2)	5.1	2.9									
At1g59610	ADL3	18 (6)	22	15				19 (7)	24	14			
At1g10290	ADL6	17 (5)	21	13				15 (3)	18	10			
At3g11130, At3g08530*	Clathrin heavy chain				6	3.6	4.1						

For both AP-3 β and AP-3 δ, two independent pull-down experiments have been performed.
N, number of different peptides (number of unique peptides); %, percentage coverage of protein; Sf, total score factor calculated by Bioworks v3.3.1. *Not distinguishable which of the two clathrin heavy chain proteins is identified.

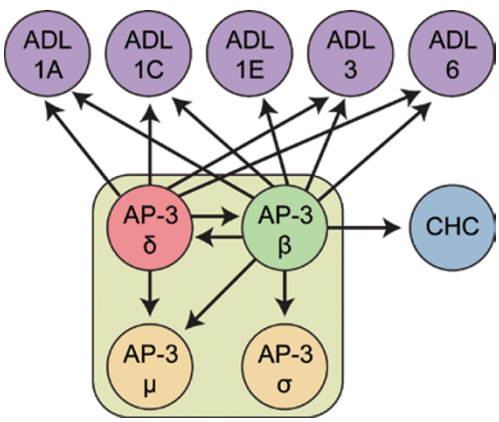

Figure 7 Schematic representation of AP-3 δ and AP-3 β interacting proteins. Immunoprecipitations using both, AP-3 δ-GFP and AP-3 β-GFP as baits identified interaction with the remaining μ and σ subunits of the AP-3 complex, as well between AP-3 δ and/or AP-3 β and *Arabidopsis* dynamin-like (ADL) and clathrin heavy chain (CHC) proteins.

complexes likely exist and act in plant cells, consisting of the same subunits as the corresponding AP complexes in yeast and animals.

Identification of AP-3 adaptor complex in plants

Striking similarity of phenotypes in mutants defective in AP-3 β, AP-3 δ or AP-3 μ as well as analysis of *pat4* × *pat2* double mutants suggest the existence of a functional AP-3 protein complex encompassing these subunits. To determine if such a complex exists in plants, and to identify which other proteins may interact with it, we generated constructs and transgenic *Arabidopsis* lines expressing AP-3 δ-GFP and AP-3 β-GFP proteins from their own promoters. We immunoprecipitated AP-3 δ-GFP as well as AP-3 β-GFP proteins from these transgenic seedlings and performed nano-LC followed by tandem mass spectrometry (nLC-MS/MS). In both cases, the GFP-tagged protein was recovered (Table 1; 73 peptides, 62% coverage for AP-3 β; 45 peptides, 53% coverage for AP-3 δ). Notably, these immunoprecipitations also recovered all three other putative subunits of the AP-3 complex from the AP-3 β-GFP line (Table 1; Figure 7). To confirm these findings, we performed a second independent experiment and found essentially the same result (Table 1; Experiment 2). This strongly suggests that the AP-3 exists in *Arabidopsis* as a complex, similarly as shown in mammalian and yeast cells [1, 7, 41, 42].

Notably, we also found clathrin heavy chain (CHC) associated with AP-3 β and several *Arabidopsis* dynamin-like proteins [43-45] associated with both AP-3 β and AP-3 δ subunits (Table 1; Figure 7). Dynamin proteins are typically involved in the formation of clathrin-coated vesicles [46-48], thus their association together with CHC with AP-3 subunits strongly supports the view that the AP-3 complex in plants could function as an adaptor complex for the formation of clathrin-coated vesicles [49].

In summary, the biochemical studies fully confirm the genetic studies that the AP-3 complex exists in plants and plays a role in clathrin- and dynamin-mediated vesicle trafficking for regulating vacuolar function.

Discussion

A fluorescence imaging-based forward genetic screen identifies putative AP-3 components

The use of forward genetic approaches for the identification of molecular components of subcellular trafficking and dynamics in plants has been limited so far, possibly due to functional redundancy of the regulators and/or lethality of corresponding mutants. The utilization of screens focused not on morphological phenotypes but on the changes in localization or dynamics in fluorescent subcellular markers has been performed to at least partially circumvent these issues and identify specifically also weak alleles or components not obviously affecting plant growth. These approaches already identified ARF GEF components of secretion [50] and endocytosis [51] and the putative AP-3 β component of vacuolar function [10]. The *pat2* mutant deficient in AP-3 β has been identified as displaying strong intracellular accumulation of PIN1-GFP. From a similar screen with an extended EMS-mutagenized population, we identified the *pat4* mutant displaying very similar cellular and morphological features as *pat2* including strong accumulation of proteins in abnormally shaped lytic vacuoles. Notably, map-based cloning revealed that *pat4* is defective in another putative AP-3 component – the putative δ adaptin. Thus, the same fluorescence-based forward genetic screen independently identified two components of the same putative AP-3 complex displaying the same phenotype. Notably, these mutants would be very difficult to recover from the conventional mutant screens as they do not display penetrant morphological or growth phenotypes.

Putative AP-3 components play similar roles in the function of vacuoles

AP-3 is a heterotetrameric protein complex that is represented in the *Arabidospis* genome by single copy genes for putative β, δ, μ and σ adaptin subunits [52]. The *pat2* mutant defective in AP-3 β, the *pat4* mutant defective in AP-3 δ and the dominant negative version of AP-3 μ that we generated all show very similar phenotypes in the morphology and function of the lytic vacuoles.

The set of defects identified in *pat2* and *pat4* mutants includes subcellular phenotypes such as altered degradation and abnormal protein accumulation in misshaped lytic vacuoles, aberrant vacuolation of PVCs and impaired transition from storage to lytic vacuoles but no defects in secretory or early endocytic processes. The mutants display largely normal morphology but arrest growth on sucrose-deficient medium. This is a feature of mutants defective in protein trafficking to the storage and/or lytic vacuoles [20, 35, 38]. In a previous study, we found abnormally sized and spherically shaped PSVs in the *pat2* embryo cells by using natural autofluorescence of storage proteins, which were confirmed by transmission electron microscopy [10]. The analysis of natural autofluorescence also revealed the abnormal morphology of PSVs in *pat4* mutants. Although *pat4* and *pat2* mutants display similar PSVs defects they do not show typical defects in trafficking of 2S albumin and 12S globulin to the PSVs. These findings reveal that *pat4-1* shows a basically identical set of defects as *pat2/ap-3 β*, a previously identified mutant from a similar screen [10], and show that *pat4-1* mutant phenotype is caused by defective vacuole biogenesis and function. Furthermore, mutants in putative AP-3 adaptins including *zig suppressor 4* (*zip4*)*/ap-3 μ*, *ap-3 δ* and *ap-3 β* all suppress the shoot gravitropism and morphology abnormalities of the *zig1/vti11* mutant that is defective in protein trafficking to the lytic vacuoles [11, 13], supporting a role of the AP-3 complex in regulating post-Golgi membrane trafficking toward the vacuole. Thus, this unique set of defects related to vacuolar functions in mutants defective in the putative AP-3 β, AP-3 δ or AP-3 μ subunits shows that putative components of the AP-3 complex play the same role in regulating biogenesis and function of vacuoles in plants.

AP-3 complex exists in plants and mediates clathrin-based trafficking for vacuolar function

Similar phenotypes of the mutants defective in the different putative subunits of the same AP-3 complex and lack of strong additive or synergistic interaction in the double mutant combination show their identical molecular function and suggest that these proteins act in the same process, possibly in the same complex. It also reveals that in analogy to yeast and animal model organisms [5, 53], the loss of either of the subunits results in the loss of the entire AP-3 complex. As all these observations strongly suggest the existence of a functional AP-3 complex in plants, we tested this hypothesis by analyzing proteins associated with β and δ putative subunits of AP-3. Importantly, from these unbiased pull-down experiments we found strongly associated proteins that constitute the remaining subunits of the AP-3 complex. Thus the biochemical studies complemented the genetic observations and confirmed that β, δ, μ and σ adaptin subunits are part of the same complex.

Notably, also several established components of vesicle formation such as adaptins and clathrin coat were found associated with these AP-3 subunits confirming the role of the AP-3 complex in vesicle formation in plant cells. The association of the plant AP-3 with clathrin would suggest that, unlike the yeast AP-3, the plant

AP-3 mediates formation of clathrin-coated vesicles, a notion that is controversial in mammalian cells [3, 7, 49, 54, 55]. Thus, the functional association of clathrin and AP-3 in the formation of vesicles in the different eukaryotes still remains unclear. However, Lee *et al*. [56] reported that in *Arabidopsis* protoplasts EpsinR2 interacts with AP-3 δ, clathrin, VTI12 and phosphatidylinositol-3-phosphate and plays roles in protein trafficking. This finding, together with our observations that AP-3 interacts with clathrin indicates that the *Arabidopsis* AP-3 complex likely functions as a clathrin adaptor complex. In mammalian cells, clathrin interaction with AP-3 is mediated by the β subunit and AP-3 β has a binding region for clathrin [49]. Accordingly, our experiments revealed association of the β but not δ subunit of the *Arabidopsis* AP-3 with clathrin. This indicates that in both mammals and higher plants, AP-3-mediated trafficking depends on the coat protein clathrin.

Nonetheless, the genetic and biochemical studies presented here demonstrate on the example of AP-3 that AP complexes exist in plant cells and play a role in vesicle formation as in other eukaryotes. Although the existence of other AP complexes in plants awaits demonstration, the AP-3 complex acquired a plant-specific function in regulating biogenesis and function of vacuoles.

Materials and Methods

Plant material and growth conditions

Seedlings of wild-type Col-0 and all mutant lines: *pat4-1* (EMS mutant), *pat4-2* (AP-3 δ SALK mutant; At1g48760; [57]), *pat2-2* (AP-3 β SAIL mutant; At3G55480, [10]), *vps29* (At3g47810, [58]), double mutant line *pat4-2* × *pat2-2*, crossed lines: *pat4-1* × PIN2-GFP, *pat4-1* × PIP2a-GFP, *pat4-1* × BRI1-GFP, *pat4-1* × GFP-RABF2b, GFP tagged lines: $PIN1_{pro}$:PIN1-GFP (At1g73590, [59]), $PIN2_{pro}$:PIN2-GFP (At5G57090; [21]), $35S_{pro}$:PIP2a-GFP (X75883, [22]), $BRI1_{pro}$:BRI1-GFP (AT4G39400, [23]), $RABF2b_{pro}$:GFP-RABF2b (AT4g19640, [34]), AP-3 β_{pro}:AP-3 β-GFP (At3G55480, [10]), AP-3 δ_{pro}:AP-3 δ-GFP (At3G55480, [56]), as well as obtained by Gateway-based cloning strategy transgenic lines: full-length Atμ3 (At1g56590) and the (18 amino acids truncated) dominant negative version were grown vertically in Petri dishes on 0.8% agar 0.5× Murashige and Skoog (MS) medium containing 1% sucrose (pH 5.9) at 18 °C, long-day photoperiod.

EMS mutagenesis, mutant forward genetic screen and mapping

M2 seedlings, progenies of 1920 M1 3% EMS-mutagenized *$PIN1_{pro}$:PIN1-GFP* plants were analyzed under an epifluorescence microscope for abnormal intracellular accumulation of PIN1-GFP signal.

pat4-1 was mapped using 300 chromosomes from the F2 progeny derived from crosses of *pat4-1* with the Landsberg *erecta* ecotype to a region of 85 kb on the lower arm of chromosome 1 (18 041-18 126; BAC F11I4), using simple sequence length polymorphism and cleaved amplified polymorphic sequence (CAPS and dCAPS) markers. For the information about Col/Ler polymorphism we used the collection of SNPs and INDELs provided by Monsanto Arabidopsis Polymorphism and Ler Sequence Collection (Cereon Genomics) and TAIR (http://www.arabidopsis.org). At1G48760 candidate gene was sequenced and we found a point mutation causing a stop codon at the position downstream of ATG.

Drug treatments and microscopy

To assess different biological processes 5-day-old seedlings were incubated in MS medium supplemented with LysoTracker red (Invitrogen; 2 μM in DMSO) and BFA (Invitrogen; 50 μM in DMSO). Control treatments were done in the same way with equivalent concentration of DMSO. For FM4-64 (Invitrogen; in H_2O) accumulation the seedlings were pulse labeled 5 min in MS liquid medium supplemented with 4 μM FM4-64 on ice, washed three times at room temperature in MS liquid medium, mounted and observed after 3 h. For the double treatments, the seedlings were first pulse labeled with 50 μM BFA and 4 μM FM4-64 as described above, followed by 1 h incubation in MS medium supplemented with 50 μM BFA. The morphology of PSVs was examined by imaging autofluorescence. Images of embryo root cells were taken immediately after peeling off the seed coat of the dry seeds. Accumulation of LysoTracker red (as described above) was done in 1 h and 60 h after imbibition. Samples were viewed by confocal laser microscopy.

Western blot and SDS-PAGE

Protein extracts were prepared from 10 dry seeds per each line in SDS-PAGE sample buffer and subjected to SDS-PAGE followed by either Coomassie blue staining or blotting to ECL membrane (GE-Healthcare) as described before [35]. The membranes were treated with antibodies against 2S albumin (rabbit; 1:5 000) and ECL™-anti-rabbit IgG, horseradish peroxidase (GE Healthcare; 1:5 000). The immunoreactive signals were detected by using the ECL detection system (GE-Healthcare).

Cloning and Arabidopsis thaliana transformation

The full-length Atμ3 (At1g56590) and the truncated dominant negative version DNA was amplified with the following primers:

attB1_Atμ3_FW GGGGACAAGTTTGTACAAAAAAGCAGGCTCGATGCTTCAATGTATCTTTCTC

attB2_Atμ3_RW GGGGACCACTTTGTACAAGAAAGCTGGGTCCTACAACCTGACATCGAACTC

attB2_Atμ3_RW-Ct GGGGACCACTTTGTACAAGAAAGCTGGGTCCTACAAACGAGGAGGGATAGTTTG.

The amplified gene was cloned under the 35S promoter. Atμ3 clones were introduced by Gateway recombination first, into pDONR221, and then into the destination vector pK7WG2,0 ([60]; http://www.psb.ugent.be/gateway).

Immunoprecipitation and liquid chromatography-mass spectrometry

For immunoprecipitation, 1.5-1.7 g of 5-day-old AP-3 β-GFP, AP-3 δ-GFP and Col-0 seedlings were ground in a mortar with liquid nitrogen. The powder was homogenized in extraction buffer (50 mM Tris-HCl, 150 mM NaCl, 1% Nonidet P-40 (NP40), protease inhibitors mix cocktail (Roche, 1 tablet per 50 ml)). After grinding, the protein extract was sonicated 3 × 15 sec with a probe sonicator (MSE) at half-maximal power and incubated on ice for

30 min. The NP40 in the protein extract was then diluted to 0.2%, followed by 2 × 15 min centrifugation at 20 000 rpm at 4 °C. The supernatant was incubated for 2 h at 4 °C with rotation with 100 µl magnetic beads coupled to a monoclonal anti-GFP antibody (Miltenyi). µColumns on a MACS MultiStand (Miltenyi) were equilibrated with 200 µl extraction buffer containing 0.1% NP40, then the supernatant was passed through the µcolumn. The column was subsequently washed with 4 × 200 µl extraction buffer containing 0.1% NP40 and 2 × 500 µl 50 mM ammoniumcarbonate. The beads were eluted from the column into low bind tubes (Eppendorf AG) with 50 µl 50 mM ammoniumcarbonate that was heated to 95 °C.

For MS measurements, 1 µl 50 mM DTT in 50 mM NH_4HCO_3 was added to the beads and incubated at 37 °C. After 2 h, 1 µl 100 mM iodocetamide in 50 mM NH_4HCO_3 was added and incubated 2 h at room temperature in the dark. Subsequently 1 µl 200 mM cysteine in 50 mM NH_4HCO_3 and 1 µl trypsin-sequencing grade (0.5 µg/µl in1 mM HCl) were added and the beads were incubated overnight at 20 °C while shaking. The following day 1.2 µl trifluoroacetic acid was added to adjust to ~pH 3 and the beads were centrifuged 3 min at maximum speed. The supernatant was subjected to nLC-MS/MS analysis using a LTQ-Orbitrap. Data were analyzed using the Bioworks software package version 3.1.1 (Thermo Scientific).

Acknowledgments

We thank Eva Benková (VIB-Ghent University, Belgium), Ben Scheres (Ulrecht University, The Netherlands), Chris R Somerville (University of California, Berkeley, USA), Niko Geldner (University of Lausanne, Swilzerland) for sharing published material, ABRC and NASC for the seed stock supply, Sjef Boeren (Biqualis, Wageningen) for help with mass spectrometry, our colleagues Stéphanie Robert and Tomasz Nodzyński for helpful discussions, suggestions and technical assistance, and Martine De Cock for help in preparing the manuscript. This work was cofinanced by the Center for BioSystems Genomics, which is part of the Netherlands Genomics Initiative/Netherlands Organization for Scientific Research (NWO), and by NWO Grant VIDI-864.06.012 (BM, DW). This work was supported by the Research Foundation-Flanders (Odysseus) for JF.

References

1 Simpson F, Bright NA, West MA, *et al*. A novel adaptor-related protein complex. *J Cell Biol* 1996; **133**:749-760.
2 Rothman JE, Wieland FT. Protein sorting by transport vesicles. *Science* 1996; **272**:227-234.
3 Drake MT, Zhu Y, Kornfeld S. The assembly of AP-3 adaptor complex-containing clathrin-coated vesicles on synthetic liposomes. *Mol Biol Cell* 2000; **11**:3723-3736.
4 Dell'Angelica EC, Mullins C, Bonifacino JS. AP-4, a novel protein complex related to clathrin adaptors. *J Biol Chem* 1999; **274**:7278-7285.
5 Cowles CR, Odorizzi G, Payne GS, *et al*. The AP-3 adaptor complex is essential for cargo-selective transport to the yeast vacuole. *Cell* 1997; **91**:109-118.
6 Stepp JD, Huang K, Lemmon SK. The yeast adaptor protein complex, AP-3, is essential for the efficient delivery of alkaline phosphatase by the alternate pathway to the vacuole. *J Cell Biol* 1997; **139**:1761-1774.
7 Dell'Angelica EC, Ohno H, Ooi CE, *et al*. AP-3: an adaptor-like protein complex with ubiquitous expression. *EMBO J* 1997; **16**:917-928.
8 Kretzschmar D, Poeck B, Roth H, *et al*. Defective pigment granule biogenesis and aberrant behavior caused by mutations in the Drosophila AP-3β adaptin gene *ruby*. *Genetics* 2000; **155**:213-223.
9 Dell'Angelica EC, Shotelersuk V, Aquilar RC, *et al*. Altered trafficking of lysosomal proteins in Hermansky-Pudlak syndrome due to mutations in the β3A subunit of the AP-3 adaptor. *Mol Cell* 1999; **3**:11-21.
10 Feraru E, Paciorek T, Feraru MI, *et al*. The AP-3 β adaptin mediates the biogenesis and function of the lytic vacuoles in *Arabidopsis*. *Plant Cell* 2010; **22**:2812-2824.
11 Niihama M, Takemoto N, Hashiguchi Y, *et al*. *ZIP* genes encode proteins involved in membrane trafficking of the TGN–PVC/vacuoles. *Plant Cell Physiol* 2009; **50**:2057-2068.
12 Surpin M, Zheng H, Morita MT, *et al*. The VTI family of SNARE proteins is necessary for plant viability and mediates different protein transport pathways. *Plant Cell* 2003; **15**:2885-2899.
13 Sanmartín M, Ordóñez A, Sohn EJ, *et al*. Divergent functions of VTI12 and VTI11 in trafficking to storage and lytic vacuoles in *Arabidopsis*. *Proc Natl Acad Sci USA* 2007; **104**:3645-3650.
14 Petrášek J, Mravec J, Bouchard R, *et al*. PIN proteins perform a rate-limiting function in cellular auxin efflux. *Science* 2006; **312**:914-918.
15 Dhonukshe P, Tanaka H, Goh T, *et al*. Generation of cell polarity in plants links endocytosis, auxin distribution and cell fate decisions. *Nature* 2008; **456**:962-966.
16 Dhonukshe P, Aniento F, Hwang I, *et al*. Clathrin-mediated constitutive endocytosis of PIN auxin efflux carriers in *Arabidopsis*. *Curr Biol* 2007; **17**:520-527.
17 Geldner N, Friml J, Stierhof Y-D, *et al*. Auxin transport inhibitors block PIN1 cycling and vesicle trafficking. *Nature* 2001; **413**:425-428.
18 Kleine-Vehn J, Dhonukshe P, Sauer M, *et al*. ARF GEF-dependent transcytosis and polar delivery of PIN auxin carriers in *Arabidopsis*. *Curr Biol* 2008; **18**:526-531.
19 Abas L, Benjamins R, Malenica N, *et al*. Intracellular trafficking and proteolysis of the *Arabidopsis* auxin-efflux facilitator PIN2 are involved in root gravitropism. *Nat Cell Biol* 2006; **8**:249-*256.*
20 Kleine-Vehn J, Leitner J, Zwiewka M, *et al*. Differential degradation of PIN2 auxin efflux carrier by retromer-dependent vacuolar targeting. *Proc Natl Acad Sci USA* 2008; **105**:17812-17817.
21 Xu J, Scheres B. Dissection of Arabidopsis ADP-RIBOSYLATION FACTOR 1 function in epidermal cell polarity. *Plant Cell* 2005; **17**:525-536.
22 Cutler SR, Ehrhardt DW, Griffitts JS, *et al*. Random GFP::cDNA fusions enable visualization of subcellular structures in cells of *Arabidopsis* at a high frequency. *Proc Natl Acad Sci USA* 2000; **97**:3718-3723.
23 Geldner N, Hyman DL, Wang X, *et al*. Endosomal signal-

ing of plant steroid receptor kinase BRI1. *Genes Dev* 2007; **21**:1598-1602.
24 Grebe M, Xu J, Möbius W, *et al*. *Arabidopsis* sterol endocytosis involves actin-mediated trafficking via ARA6-positive early endosomes. *Curr Biol* 2003; **13**:1378-1387.
25 Dettmer J, Hong-Hermesdorf A, Stierhof Y-D, *et al*. Vacuolar H^+-ATPase activity is required for endocytic and secretory trafficking in *Arabidopsis*. *Plant Cell* 2006; **18**:715-730.
26 Robinson DG, Jiang L, Schumacher K. The endosomal system of plants: charting new and familiar territories. *Plant Physiol* 2008; **147**:1482-1492.
27 Jelínková A, Malínská K, Simon S, *et al*. Probing plant membranes with FM dyes: tracking, dragging or blocking? *Plant J* 2010; **61**:883-892.
28 Ueda T, Yamaguchi M, Uchimiya H, *et al*. Ara6, a plant-unique novel type Rab GTPase, functions in the endocytic pathway of *Arabidopsis thaliana*. *EMBO J* 2001; **20**:4730-4741.
29 Laxmi A, Pan J, Morsy M, *et al*. Light plays an essential role in intracellular distribution of auxin efflux carrier PIN2 in *Arabidopsis thaliana*. *PLoS ONE* 2008; **3**:e1510.
30 Marty F. Plant vacuoles. *Plant Cell* 1999; **11**:587-599.
31 Sanderfoot AA, Ahmed SU, Marty-Mazars D, *et al*. A putative vacuolar cargo receptor partially colocalizes with AtPEP12p on a prevacuolar compartment in *Arabidopsis* roots. *Proc Natl Acad Sci USA* 1998; **95**:9920-9925.
32 Tse YC, Mo B, Hillmer S, *et al*. Identification of multivesicular bodies as prevacuolar compartments in *Nicotiana tabacum* BY-2 cells. *Plant Cell* 2004; **16**:672-693.
33 daSilva LLP, Taylor JP, Hadlington JL, *et al*. Receptor salvage from the prevacuolar compartment is essential for efficient vacuolar protein targeting. *Plant Cell* 2005; **17**:132-148.
34 Jaillais Y, Fobis-Loisy I, Miège C, Rollin C, Gaude T. AtSNX1 defines an endosome for auxin-carrier trafficking in *Arabidopsis*. *Nature* 2006; **443**:106-109.
35 Shimada T, Koumoto Y, Li L, *et al*. AtVPS29, a putative component of a retromer complex, is required for the efficient sorting of seed storage proteins. *Plant Cell Physiol* 2006; **47**:1187-1194.
36 Silady RA, Ehrhardt DW, Jackson K, *et al*. The GRV2/RME-8 protein of Arabidopsis functions in the late endocytic pathway and is required for vacuolar membrane flow. *Plant J* 2008; **53**:29-41.
37 Isono E, Schwechheimer C. Co-immunoprecipitation and protein blots. In: Hennig L, Köhler C, eds. *Plant Developmental Biology: Methods and Protocols, Methods in Molecular Biology,* Vol 655. Totowa: Humana Press, 2010:377-387.
38 Ebine K, Okatani Y, Uemura T, *et al*. A SNARE complex unique to seed plants is required for protein storage vacuole biogenesis and seed development of *Arabidopsis thaliana*. *Plant Cell* 2008; **20**:3006-3021.
39 Owen DJ, Evans PR. A structural explanation for the recognition of tyrosine-based endocytotic signals. *Science* 1998; **282**:1327-1332.
40 Nesterov A, Carter RE, Sorkina T, *et al*. Inhibition of the receptor-binding function of clathrin adaptor protein AP-2 by dominant-negative mutant μ2 subunit and its effects on endocytosis. *EMBO J* 1999; **18**:2489-2499.
41 Dell'Angelica EC, Ooi CE, Bonifacino JS. β3A-adaptin, a subunit of the adaptor-like complex AP-3. *J Biol Chem* 1997; **272**:15078-15084.
42 Panek HR, Stepp JD, Engle HM, *et al*. Suppressors of *YCK*-encoded yeast casein kinase 1 deficiency define the four subunits of a novel clathrin AP-like complex. *EMBO J* 1997; **16**:4194-4204.
43 Park JM, Kang SG, Pih KT, *et al*. A dynamin-like protein, ADL1, is present in membranes as a high-molecular-mass complex in *Arabidopsis thaliana*. *Plant Physiol* 1997; **115**:763-771.
44 Konopka CA, Backues SK, Bednarek SY. Dynamics of *Arabidopsis* dynamin-related protein 1C and a clathrin light chain at the plasma membrane. *Plant Cell* 2008; **20**:1363-1380.
45 Bednarek SY, Backues SK. Plant dynamin-related protein families DRP1 and DRP2 in plant development. *Biochem Soc Trans* 2010; **38**:797-806.
46 Damke H, Baba T, Warnock DE, *et al*. Induction of mutant dynamin specifically blocks endocytic coated vesicle formation. *J Cell Biol* 1994; **127**:915-934.
47 Sever S, Damke H, Schmid SL. Dynamin:GTP controls the formation of constricted coated pits, the rate limiting step in clathrin-mediated endocytosis. *J Cell Biol* 2000; **150**:1137-1147.
48 Hill E, van der Kaay J, Downes CP, *et al*. The role of dynamin and its binding partners in coated pit invagination and scission. *J Cell Biol* 2001; **152**:309-323.
49 Dell'Angelica EC, Klumperman J, Stoorvogel W, *et al*. Association of the AP-3 adaptor complex with clathrin. *Science* 1998; **280**:431-434.
50 Teh OK, Moore I. An ARF-GEF acting at the Golgi and in selective endocytosis in polarized plant cells. *Nature* 2007; **448**:493-496.
51 Tanaka H, Kitakura S, De Rycke R, *et al*. Fluorescence imaging-based screen identifies ARF GEF component of early endosomal trafficking. *Curr Biol* 2009; **19**: 391-397.
52 Bassham DC, Brandizzi F, Otegui MS, Sanderfoot AA. The secretory system of *Arabidopsis*. *Arabidopsis Book* 2008; **6**:e0116.
53 Boehm M, Bonifacino JS. Genetic analyses of adaptin function from yeast to mammals. *Gene* 2002; **286**:175-186.
54 Simpson F, Peden AA, Christopoulou L, *et al*. Characterization of the adaptor-related protein complex, AP-3. *J Cell Biol* 1997; **137**:835-845.
55 Faúndez V, Horng JT, Kelly RB. A function for the AP3 coat complex in synaptic vesicle formation from endosomes. *Cell* 1998; **93**:423-432.
56 Lee GJ, Kim H, Kang H, *et al*. EpsinR2 interacts with clathrin, adaptor protein-3, AtVTI12, and phosphatidylinositol-3-phosphate. Implications for epsinR2 function in protein trafficking in plant cells. *Plant Physiol* 2007; **143**:1561-1575.
57 Alonso JM, Stepanova AN, Leisse TJ, *et al*. Genome-wide insertional mutagenesis of *Arabidopsis thaliana*. *Science* 2003; **301**:653-657.
58 Jaillais Y, Santambrogio M, Rozier F, *et al*. The retromer protein VPS29 links cell polarity and organ initiation in plants. *Cell* 2007; **130**:1057-1070.
59 Benková E, Michniewicz M, Sauer M, *et al*. Local, efflux-dependent auxin gradients as a common module for plant organ formation. *Cell* 2003; **115**:591-602.

60 Karimi M, Inzé D, Depicker A. GATEWAY vectors for *Agrobacterium*-mediated plant transformation. *Trends Plant Sci* 2002; **7**:193-195.

(**Supplementary information** is linked to the online version of the paper on the *Cell Research* website.)